Direct Observation of C_2 Hydrocarbon−Oxygen Complexes on Ag(110) with a Variable-Low-Temperature Scanning Tunneling Microscope

J. R. Hahn* and W. Ho

Department of Physics and Astronomy and Department of Chemistry, University of California, Irvine, California 92697-4575

Received: March 18, 2005; In Final Form: August 3, 2005

A variable-low-temperature scanning tunneling microscope (STM) was used to observe oxygen (O_2), ethylene (C_2H_4), and acetylene (C_2H_2) molecules on a Ag(110) surface and the various complexes that were formed between these two hydrocarbons and oxygen at 13 K. Ethylene molecule(s) were moved to the vicinity of O_2 either by STM tunneling electrons at 13 K or thermally at 45 K to form $(C_2H_4)_x$−O_2 ($x = 1-4$) complexes stabilized by C−H···O hydrogen bonding. Acetylene−oxygen complexes involving one or two acetylene molecules were observed.

The heterogeneous selective oxidation of hydrocarbons is a topic of enormous industrial importance and has therefore been extensively studied. Most thermodynamically favorable hydrocarbon oxidation reactions give rise to undesirable products such as CO_2 and H_2O;[1−3] hence, achieving acceptable selectivity in hydrocarbon oxidation is particularly important in industrial processes. Selectivity with respect to the formation of useful partial oxide (intermediates) can only be accomplished via kinetic control; however, such control requires a good understanding of the surface reaction mechanisms.[1,4] Most previous studies of hydrocarbon oxidation have been performed at silver surfaces because silver-catalyzed partial oxidation of hydrocarbons, in particular, epoxidation (ethylene to ethylene oxide), is the most widely exploited catalytic oxidation reaction on an industrial scale.[5] Achieving a molecular level understanding of the epoxidation mechanism is arguably the most important challenge in this field.[6−10] Thus, to enhance the basic knowledge on hydrocarbon catalytic oxidation reactions, we carried out molecular scale imaging of the complexes formed between an oxygen molecule and C_2 hydrocarbons (ethylene or acetylene) on the silver surface using a scanning tunneling microscope.

An interesting aspect of hydrocarbon oxidation is its uniqueness: not only is silver the only metal that catalyzes the epoxidation reaction but also ethylene is the only hydrocarbon that is epoxidized with high selectivity (up to 80%).[11,12] Olefins such as propylene,[11,13] styrene,[14] 3,3-dimethylbutene,[15] norborene,[16] and butadiene are also epoxidized on a silver surface but with very low selectivities (below 5%).[11,13] Other molecules such as butenes and penetenes are mainly combusted into CO_2 and H_2O.[17] Alkynes (acetylene and propyne) also undergo complete oxidation; no epoxides have been observed to form on a silver surface.[18,19] In addition, the identity of the adsorbed oxygen species responsible for the ethylene epoxidation and combustion has been the subject of a long-standing controversy. Three mechanisms have been put forward for epoxidation at a silver surface, involving surface molecular oxygen,[20−23] atomic oxygen,[24−28] and subsurface oxygen[26] as the active species. Thus, three main factors appear to affect the mechanism by which hydrocarbons are oxidized at metal surfaces: the metal used, the structure of the hydrocarbon, and the identity of oxygen species. Despite numerous reports on the epoxidation on silver, an understanding of the complete reaction pathway is still required.

In this paper, we present scanning tunneling microscopy (STM) images of hydrocarbon−O_2 complexes formed on Ag(110) after one or more ethylene or acetylene molecules had been manipulated into the vicinity of an oxygen molecule on the silver surface either with tunneling electrons (at 13 K) or thermally (at 45 K). Elucidation of the characteristics of these complexes may provide insights into the fundamental mechanisms of hydrocarbon chemistry.

Experiments were performed using a homemade, variable-temperature STM,[29] housed inside an ultrahigh vacuum chamber with a base pressure of 2×10^{-11} Torr (2.7×10^{-9} Pa). The Ag(110) sample was prepared by 500 eV neon ion sputtering followed by annealing at 693 K. Polycrystalline tungsten tips were prepared in situ by self-sputtering and annealing. Adsorbates were introduced into the chamber via a capillary array doser attached to a variable leak valve. The O_2 molecules were adsorbed on the sample at 45 K to ensure molecular chemisorption. The O_2 coverage was kept below 0.01 monolayer (ML) to permit investigation of individual well-isolated molecules. Coadsorption of ethylene and acetylene molecules onto the Ag(110) surface at coverages of less than 0.01 ML was performed at either 13 or 45 K. Atomically resolved imaging was achieved by transferring an ethylene molecule to the tip at 13 K.[30]

Figure 1a shows a constant-current STM image taken with a bare metallic tip of one physisorbed ethylene and two chemisorbed oxygen molecules. The ethylene molecule appears as an oval-shaped protrusion elongated along the [001] direction on Ag(110) under typical imaging conditions, while the oxygen molecules appear as an oval-shaped depression elongated along the $[1\bar{1}0]$ direction. Atomically resolved imaging the same area using an ethylene-terminated tip (Figure 1b) established that ethylene binds at the atop site, in agreement with previous theoretical calculations.[31] Previous studies have examined the structures of ethylene adsorbed on Ag(110) surfaces.[32−37] Using high-resolution electron energy spectroscopy (HREELS), Backx et al.[32−34] revealed that (i) ethylene adsorbs onto Ag(110)

* To whom correspondence should be addressed. Department of Chemistry, Chonbuk National University, Jeonju 561-756, Korea. E-mail: jrhahn@chonbuk.ac.kr.

10.1021/jp051431c CCC: $30.25
Published on Web 10/07/2005

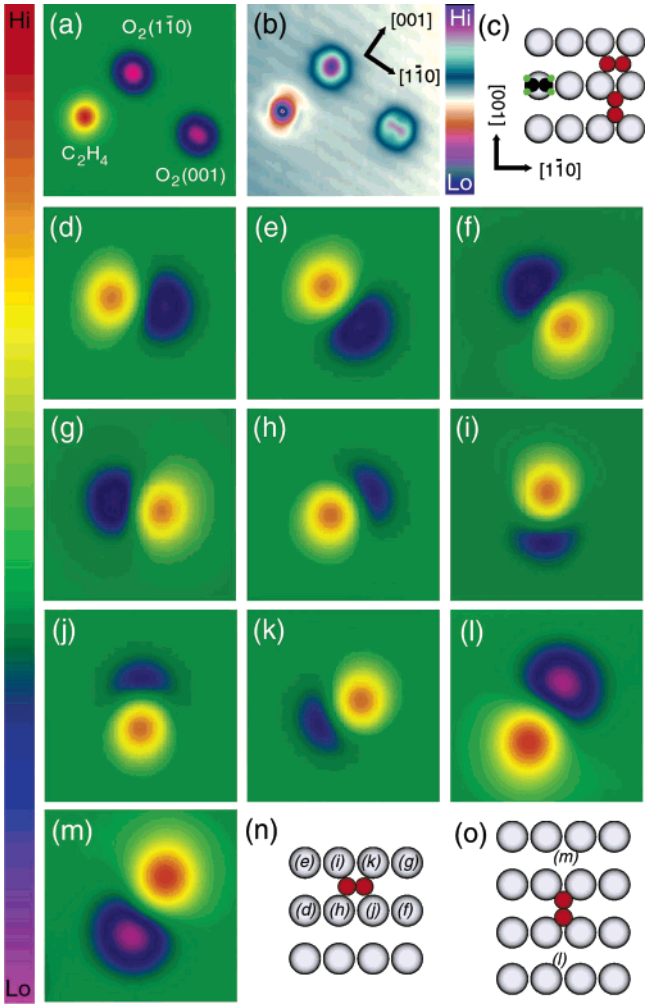

Figure 1. STM topographical images of C_2H_4, O_2 molecules, and $C_2H_4-O_2$ complexes on Ag(110), obtained at 70 mV sample bias and 1 nA tunneling current. (a) Image of one C_2H_4 molecule and two types of chemisorbed O_2 molecules obtained with a bare metallic tip. The C_2H_4 (O_2) appears as an elongated protrusion (depression) along the [001] ([1$\bar{1}$0]) direction. The O−O axis of each O_2 is parallel to the surface and oriented either along the [001] direction [O_2(001)] or along the [1$\bar{1}$0] direction [O_2(1$\bar{1}$0)]. (b) An atomically resolved image obtained with a C_2H_4-terminated tip. Grid lines are drawn through the silver surface atoms. (c) Schematic diagram for the adsorption sites of the molecules. The sizes of the circles are scaled to the atomic covalent radii of H (green), C (black), O (red), and Ag (gray). Scan area is 44 Å × 44 Å. The C_2H_4 was moved to the O_2(1$\bar{1}$0) by repeated sample voltage pulses (+250 mV at 1 nA tunneling current set), which led to the formation of the $C_2H_4-O_2$(1$\bar{1}$0) complexes, d−k. The ethylene can sit on the next-nearest-neighbor atop site ($C_2H_4^{nnnt}-O_2$(1$\bar{1}$0), d−g) or the nearest-neighbor atop site ($C_2H_4^{nnt}-O_2$(1$\bar{1}$0), h−k). Movement of the C_2H_4 to the O_2(001) can lead to the formation of $C_2H_4-O_2$(001) shown in l and m. See the text for details. Scan area for each image (d−m) is 23 Å × 23 Å. (n) Schematic diagram for images d−k indicating the ethylene adsorption position. (o) Schematic diagram for images l and m. Full scale of the *z*-axis bar on the left column is 0.9 Å.

surfaces via a weak bonding with its C═C axis parallel to the surface, (ii) the adsorption is strongly promoted by the presence of adsorbed oxygen, and (iii) ethylene adsorbs selectively onto silver atoms on which a positive charge has been induced by the oxygen atoms. The C−C axis may be aligned preferentially along the [1$\bar{1}$0] direction, as shown schematically in Figure 1c. Theoretical calculations[36] predict that adsorption of ethylene is 0.02 eV more favorable when the ethylene molecular axis is parallel to the [1$\bar{1}$0] direction compared to the [001] direction.

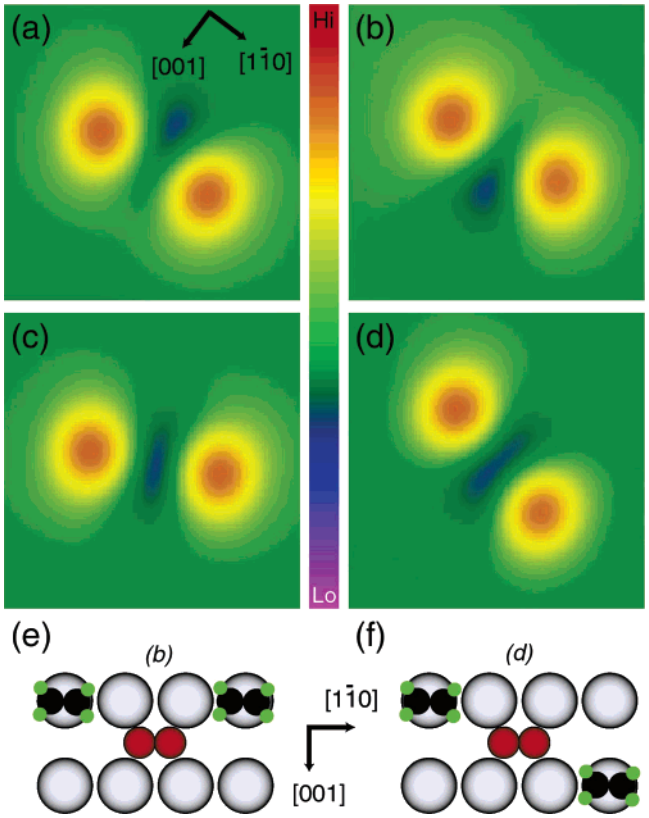

Figure 2. Movement of C_2H_4 to the $C_2H_4-O_2$(1$\bar{1}$0) complex leads to the formation of the $(C_2H_4)_2-O_2$(1$\bar{1}$0) complexes, a−d. In these complexes, the ethylene molecules reside on two of the four equivalent nnnt sites from the O_2, resulting in four $(C_2H_4)^{nnnt}{}_2-O_2$(1$\bar{1}$0) configurations. The images were obtained with a bare tip at 70 mV sample bias and 1 nA tunneling current. Scan area is 25 Å × 25 Å. (e) and (f) Schematic diagrams for images b and d.

Two predominant types of chemisorbed O_2 have been identified,[38,39] one with the molecular axis aligned along the [001] direction of the substrate [O_2(001)] and the other with the molecular axis aligned along the [1$\bar{1}$0] direction [O_2(1$\bar{1}$0)] (Figure 1c). We note that the O_2(1$\bar{1}$0) molecule is slightly more depressed than the O_2(001) molecule in the topographical image. The O_2(001) irreversibly rotates to the O_2(1$\bar{1}$0) by applying a bias voltage pulse.[38]

The ethylene molecule is weakly adsorbed on Ag(110), which enables a precise manipulation both vertically (between the STM tip apex and the surface) and laterally (on the surface) by maintaining the appropriate sample bias voltage and tunneling current at a substrate temperature of 13 K. For vertical transfer from the surface to the tip,[30] the bare metallic tip was positioned over an ethylene molecule with the junction set by a tunneling current of 0.1 nA and a sample bias voltage of +70 mV. While the feedback loop was kept on, the bias was flipped to −70 mV and then decreased to −140 mV. The tunneling current was then ramped from 0.1 to 10 nA to induce the transfer of ethylene to the tip. The resulting ethylene-terminated tip can then be used for atomically resolved imaging (Figure 1b). The enhanced spatial resolution achieved using this tip may be attributed to either overlap between the spatially localized molecular orbital of the ethylene at the tip apex with the electronic states at the surface or the higher resistivity of the ethylene on the tip compared to the bare tip.

The ethylene was moved laterally at 13 K by applying a positive sample voltage pulse of ∼250 mV with feedback off after setting the tunneling gap over the molecule at a sample bias voltage of 70 mV and a tunneling current of 1 nA. The

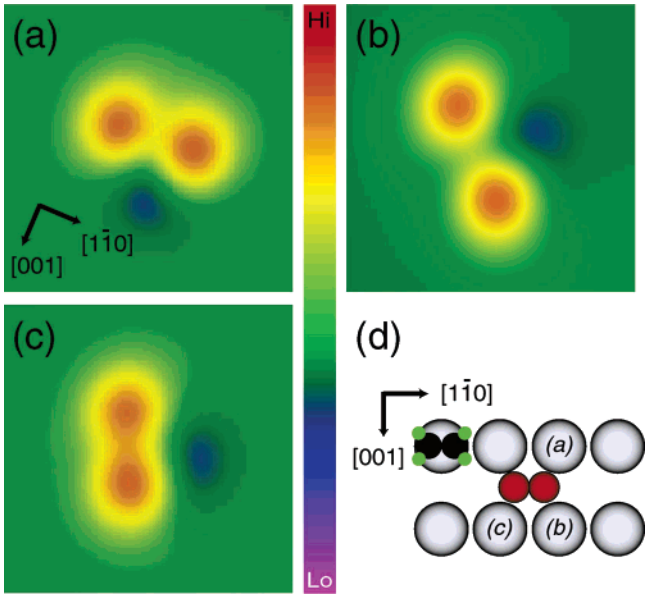

Figure 3. Injection of tunneling electrons (~200 meV at 1 nA tunneling current) on the C_2H_4 of the $(C_2H_4)^{nnnt}{}_2-O_2(1\bar{1}0)$ (Figure 2) leads to the formation of different configurations of the two-ethylene complexes. One C_2H_4 moves closer to the $O_2(1\bar{1}0)$ to form the $C_2H_4{}^{nnnt}-O_2(1\bar{1}0)-C_2H_4{}^{nnt}$ complexes (a−c). (d) Schematic diagrams for a−c. Twelve configurations were observed for this type of complex. The images were obtained with a bare tip at 70 mV sample bias and 1 nA tunneling current. Scan area is 25 Å × 25 Å.

ethylene was moved adjacent to the $O_2(1\bar{1}0)$ molecule by applying repeated sample voltage pulses, leading to the formation of a $C_2H_4-O_2(1\bar{1}0)$ complex. Eight configurations of this complex were observed (parts d−k of Figure 1). In these complexes, the ethylene adsorption position is assigned to either the nearest-neighbor atop site (nnt, parts h−k of Figure 1) or the next-nearest-neighbor atop site (nnnt, parts d−g of Figure 1). The ethylene can also be moved thermally at an elevated temperature (when dosed at 45 K), leading to the spontaneous formation of the same eight $C_2H_4-O_2(1\bar{1}0)$ complexes shown in parts d−k of Figure 1. The nnt ethylenes are slightly less prominent than the nnnt ethylenes in the topographical images. At 45 K, the same complexes can be produced by thermal diffusion of ethylenes: 84.6% of the complexes are formed in the nnnt configurations and 15.4% in the nnt configurations, as determined by sampling 400 complexes. This population distribution suggests that the nnnt geometry is thermodynamically more stable than the nnt geometry (by 6 meV assuming that an equilibrium is reached in our experiment). The isomerization barrier between the two geometries may be higher than 45 K.

The ethylene can also be moved adjacent to the $O_2(001)$, leading to the formation of the $C_2H_4-O_2(001)$ complex (Figures 1l and 1m) as well as the $C_2H_4-O_2(1\bar{1}0)$ complexes (parts d−k of Figure 1). In the $C_2H_4-O_2(001)$ complex, the ethylene adsorption position is assigned to near the next-nearest-neighbor fourfold hollow site (ffh, Figures 1l and 1m). Applying sample bias voltage pulses over the $C_2H_4-O_2(001)$ complex can induce the formation of the $C_2H_4-O_2(1\bar{1}0)$ complex; thus, both ethylene and O_2 change their adsorption geometry during this process. The formation of the $C_2H_4-O_2(1\bar{1}0)$ complex by moving ethylene into the vicinity of $O_2(001)$ indicates that $O_2(001)$ can rotate upon complex formation. The change from $C_2H_4-O_2(001)$ to $C_2H_4-O_2(1\bar{1}0)$ is irreversible, which suggests that the $C_2H_4-O_2(1\bar{1}0)$ configuration is thermodynamically more stable. Moreover, within the $C_2H_4-O_2(1\bar{1}0)$ complex, the ethylene can

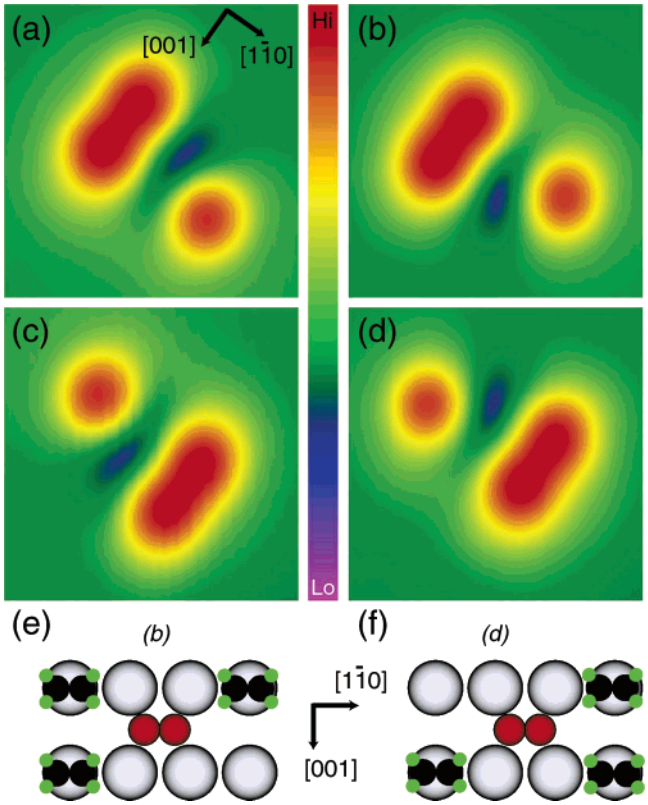

Figure 4. Attachment of a third ethylene to the $(C_2H_4)_2-O_2$ complex (Figures 2 and 3) to give a three-ethylene complex. The three ethylene molecules can sit on three of the four equivalent nnnt sites to form four $(C_2H_4)^{nnnt}{}_3-O_2(1\bar{1}0)$ configurations (a−d). (e) and (f) Schematic diagrams for b and d, respectively. The images were obtained with a bare tip at 70 mV sample bias and 1 nA tunneling current. Scan area is 25 Å × 25 Å.

be translocated around the $O_2(1\bar{1}0)$ by applying sample voltage pulses. The $C_2H_4-O_2(001)$ complexes were observed only at 13 K by manipulation with sample voltage pulses; they did not form at 45 K. Thus, it appears that the $C_2H_4-O_2(001)$ complex is a metastable configuration with a low energy barrier for conversion to the $C_2H_4-O_2(1\bar{1}0)$ complex.

The orientation of O_2 molecules of the complexes was determined by using STM inelastic electron tunneling spectroscopy (STM-IETS). A study of the $C_2H_4-O_2(001)$ and $C_2H_4-O_2(1\bar{1}0)$ complexes using STM-IETS revealed that the $O_2(001)$ of the $C_2H_4-O_2(001)$ complexes exhibits two vibrational modes, whereas the $C_2H_4-O_2(1\bar{1}0)$ complexes exhibit no such modes.[40] In our previous STM-IETS study of O_2, it was shown that isolated $O_2(001)$ but not $O_2(1\bar{1}0)$ gives rise to vibrational modes.[39]

Complexes involving two ethylenes and one oxygen can also be created by moving an additional ethylene into the vicinity of the $C_2H_4-O_2(1\bar{1}0)$ complex to form the two types of $(C_2H_4)_2-O_2(1\bar{1}0)$ complexes shown in Figures 2 and 3. In the complex shown in Figure 2, both ethylene molecules are bonded to nnnt sites ($(C_2H_4)^{nnnt}{}_2-O_2(1\bar{1}0)$), whereas the complex shown in Figure 3 consists of one nnt and one nnnt ethylene ($C_2H_4{}^{nnnt}-O_2(1\bar{1}0)-C_2H_4{}^{nnt}$). Four types of geometrical configuration were observed for the former and twelve types for the latter. In these configurations, the two ethylenes do not reside on neighboring Ag atoms due to the repulsive interaction between the ethylene molecules. The $(C_2H_4)^{nnnt}{}_2-O_2(1\bar{1}0)$ complex could be changed to the $C_2H_4{}^{nnnt}-O_2(1\bar{1}0)-C_2H_4{}^{nnt}$ complex by applying sample voltage pulses, but the reverse was not observed.

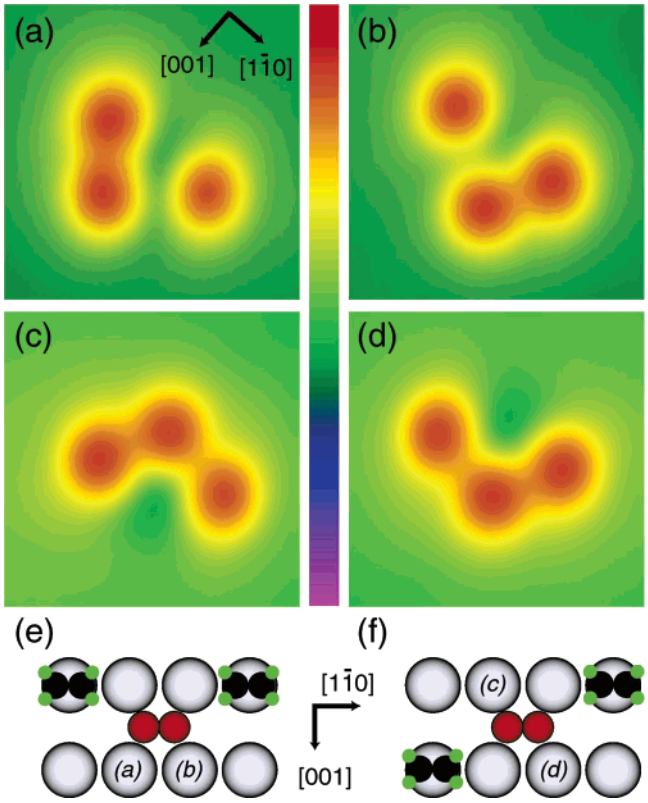

Figure 5. Movement of one ethylene of the $(C_2H_4)^{nnnt}{}_3-O_2(1\bar{1}0)$ complex (Figure 4) to a nnt site by 200 meV tunneling electrons gives rise to eight $(C_2H_4)^{nnnt}{}_2-O_2(1\bar{1}0)-C_2H_4{}^{nnt}$ configurations (four shown in a−d). (e) and (f) Schematic diagrams for configurations a−d. The images were obtained with a bare tip at 70 mV sample bias and 1 nA tunneling current. Scan area is 25 Å × 25 Å.

Attachment of three ethylene molecules to the $O_2(1\bar{1}0)$ led to the formation of either $(C_2H_4)^{nnnt}{}_3-O_2(1\bar{1}0)$ (Figure 4) or $(C_2H_4)^{nnnt}{}_2-O_2(1\bar{1}0)-C_2H_4{}^{nnt}$ (Figure 5), with four geometrical configurations being observed for each type. Further, attachment of four ethylene molecules to the $O_2(1\bar{1}0)$ gave rise to the complexes shown in Figure 6, in which either all ethylene molecules are bonded to nnnt sites ($(C_2H_4)^{nnnt}{}_4-O_2(1\bar{1}0)$, Figure 6a) or two ethylenes are bonded to nnnt sites and two to nnt sites ($(C_2H_4)^{nnnt}{}_2-O_2(1\bar{1}0)-(C_2H_4)^{nnt}{}_2$, Figure 6b). Only one configuration was observed for the former complex and two configurations for the latter complex.

In the gas phase, the interaction between O_2 and ethylene is so weak that the molecules do not form complexes. The present STM results and previous ab initio density functional theory calculations[31] indicate that the complexes formed between O_2 and ethylene on a silver substrate are stabilized by hydrogen bonding between a C−H group of the ethylene and O_2. The calculated bond distances ($d_{C-H\cdots O}$) are 2.79 and 2.76 Å for $C_2H_4{}^{nnnt}-O_2(1\bar{1}0)$ and $C_2H_4{}^{nnt}-O_2(1\bar{1}0)$, respectively.[31] These hydrogen bonds result from adsorption-induced electron transfer to the O_2, which enhances the electrostatic interaction between the oxygen molecule and the hydrogen of ethylene.

Figure 7 shows the complexes formed between acetylene and $O_2(1\bar{1}0)$ at 13 K; acetylene is highly mobile even at 13 K and spontaneously diffuses to the $O_2(1\bar{1}0)$ to form complexes. Either one (parts a and b of Figure 7) or two (Figure 7c) acetylene molecules can bind to the $O_2(1\bar{1}0)$. The adsorption position of the acetylene of the complex is determined to the nearest-neighbored fourfold hollow site by high-resolution imaging using an ethylene-terminated tip. The acetylene in the monoacetylene complex can be translocated around the $O_2(1\bar{1}0)$ by

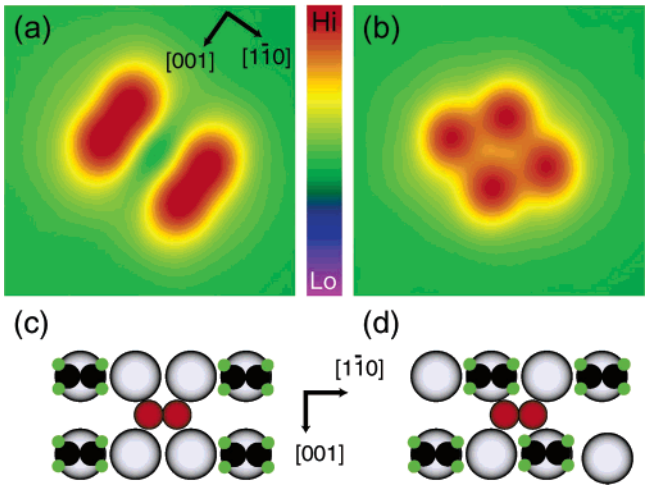

Figure 6. Four ethylene molecules can bind to an $O_2(1\bar{1}0)$ molecule to form (a) a $(C_2H_4)^{nnnt}{}_4-O_2(1\bar{1}0)$ complex or (b) a $(C_2H_4)^{nnnt}{}_2-O_2(1\bar{1}0)-(C_2H_4)^{nnt}{}_2$ complex. One configuration was observed for the former and two for the latter. $(C_2H_4)^{nnnt}{}_2-O_2(1\bar{1}0)-(C_2H_4)^{nnt}{}_2$ complexes were formed upon the injection of tunneling electrons onto the ethylene of the $(C_2H_4)^{nnnt}{}_4-O_2(1\bar{1}0)$ complex. (c) and (d) Schematic diagrams for a and b, respectively. The images were obtained with a bare tip at 70 mV sample bias and 1 nA tunneling current. Scan area is 25 Å × 25 Å.

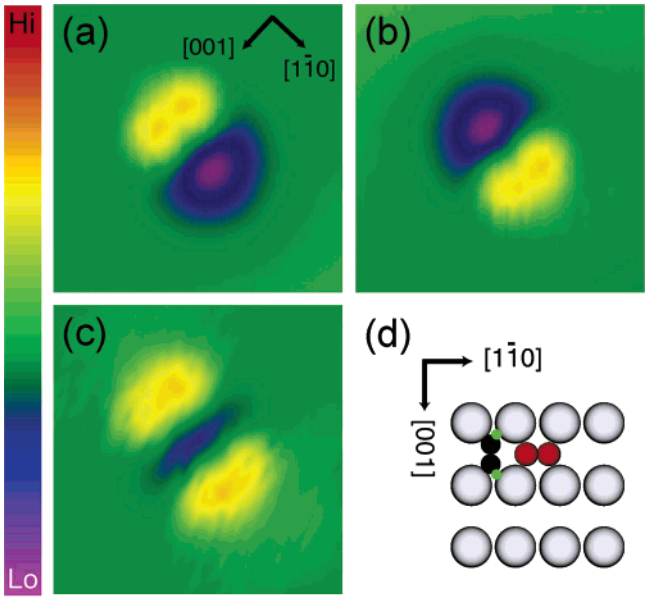

Figure 7. STM topographical images of (a) $C_2H_2-O_2(1\bar{1}0)$ and (b) $(C_2H_2)_2-O_2(1\bar{1}0)$ complexes. Two distinct configurations were observed for a and for b. These complexes were formed by thermal diffusion of acetylene upon adsorption at 13 K. (d) Schematic diagram for complex a. The images were obtained with a bare tip at 70 mV sample bias and 0.1 nA tunneling current. Scan area is 25 Å × 25 Å.

applying sample voltage pulses. In these images, the acetylenes in the complexes appear blurry and with two prominences, possibly due to fluctuation of the hydrogen atoms.

The hydrogen bond strength depends on the hybridization of the donor carbon atom and the acidity of the donor C−H group according to the calculations.[41] Generally, the sp hybridization of alkynes allows the C−H group to form a more attractive interaction with a proton acceptor, rather than alkenes.[42] On a solid surface, however, the adsorption geometry should be also considered. When acetylene is adsorbed on Ag(110), its hydrogen atoms are not directed parallel to the surface, which may disturb the formation of hydrogen bonds.

In summary, we first observed various configurations of the $(C_2H_4)_x-O_2$ ($x = 1-4$) and $(C_2H_2)_x-O_2$ ($x = 1$ and 2) complexes adsorbed on Ag(110). In these complexes, ethylene is bound to O_2 through C−H···O hydrogen bonds. An initial pathway for the reactants can be an important factor for the epoxidation and combustion reactions. Our observations, which may be involved in the initial states of either epoxidation or complete oxidation reaction pathways, provide an excellent starting point for the theoretical understanding aimed at elucidating the selectivity of oxidation reactions at silver surfaces.

Acknowledgment. This paper is based upon work supported by the Chemical Science, Geo- and Bioscience Division, Office of Science, U.S. Department of Energy (Grant DE-FG03-01ER15157). We are grateful to Hyojune Lee for assistance with the experimental apparatus.

References and Notes

(1) Haber, J. In *Handbook of Heterogeneous Catalysis*; Ertl, G., Knozinger, H., Weitkamp, J., Eds.; VCH: Weinheim, Germany, 1997; p 2253.
(2) Mavrikakis, M.; Barteau, M. A. *J. Mol. Catal. A* **1998**, *131*, 135.
(3) Madix, R. J.; Roberts, J. T. In *Surface Reactions, Springer Series Surface Sciences*; Madix, R. J., Ed.; Springer-Verlag: Berlin, 1994; Vol. 34, p 5.
(4) Zaera, F. *Acc. Chem. Res.* **2002**, *35*, 129.
(5) van Santen, R. A.; Kuipers, H. P. C. *Adv. Catal.* **1987**, *35*, 265.
(6) Zaera, F. J. *Phys. Chem. B* **2002**, *106*, 4043.
(7) Bocquet, M.-L.; et al. *J. Am. Chem. Soc.* **2003**, *125*, 5620.
(8) Medlin, J. W.; Barteau, M. A. *J. Phys. Chem.* **2001**, *105*, 10054.
(9) Linic, S.; Barteau, M. A. *J. Am. Chem. Soc.* **2002**, *124*, 310.
(10) Linic, S.; Piao, H.; Adib, K.; Barteau, M. A. *Angew. Chem., Int. Ed.* **2004**, *43*, 2918.
(11) Kilty, P. A.; Sachtler, W. M. H. *Catal. Rev.−Sci. Eng.* **1974**, *10*, 1.
(12) Voge, H. H.; Adams, C. R. *Adv. Catal.* **1967**, *17*, 151.
(13) Cant, N. W.; Hall, W. K. *J. Catal.* **1978**, *52*, 81.
(14) Hawker, S.; Mukoid, C.; Badyal, J. P. S.; Lambert, R. M. *Surf. Sci.* **1989**, *219*, L615.
(15) Mukoid, C.; Hawker, S.; Badyal, J. P. S.; Lambert, R. M. *Catal. Lett.* **1990**, *4*, 57.
(16) Roberts, J. T.; Madix, R. J. *J. Am. Chem. Soc.* **1988**, *110*, 8540.
(17) Akimoto, M.; Ichikawa, K.; Echigoya, E. *J. Catal.* **1982**, *76*, 333.
(18) Barteau, M. A.; Madix, R. J. *Surf. Sci.* **1982**, *115*, 355.
(19) Vohs, J. M.; Carney, B. A.; Barteau, M. A. *J. Am. Chem. Soc.* **1985**, *107*, 7841.
(20) Henriques, C.; Portela, M. F.; Mazzocchia, C.; Guglielminotti, E. In *New Frontiers in Catalysis*; Guczi, J., et al., Eds.; 1993; pp 1995−1998.
(21) Campbell, C. T. *J. Catal.* **1986**, *99*, 28.
(22) Campbell, C. T.; Paffett, M. T. *Surf. Sci.* **1986**, *177*, 417.
(23) Portela, M. F.; Henriques, C.; Pires, M. J.; Ferreria, J.; Baerna, M. *Catal. Today* **1987**, *1*, 101.
(24) Force, E. L.; Bell, A. T. *J. Catal.* **1985**, *40*, 364.
(25) Gleaves, J. T.; Sault, A. G.; Madix, R. J.; Ebner, J. R. *J. Catal.* **1990**,*121*, 202.
(26) van den Hoek, P. J.; Baerends, E. J.; van Santen, R. A. *J. Phys. Chem.* **1989**, *93*, 6469.
(27) Jorgensen, K. A.; Hoffmann, R. *J. Phys. Chem.* **1990**, *94*, 3406.
(28) Barteau, M. A.; Madix, R. J. *J. Am. Chem. Soc.* **1983**, *105*, 344.
(29) The STM is a variation of the one described in Stipe, B. C.; Rezaei, M. A.; Ho, W. *Rev. Sci. Instrum.* **1999**, *70*, 137. Lauhon, L. J.; Ho, W. *Rev. Sci. Instrum.* **2001**, *72*, 216.
(30) Hahn, J. R.; Ho, W. *Phys. Rev. Lett.* **2001**, *87*, 196102.
(31) Gao, S.; Hahn, J. R.; Ho, W. *J. Chem. Phys.* **2003**, *119*, 6232.
(32) Backx, C.; de Groot, C. P. M.; Biloen, P. *Appl. Surf. Sci.* **1980**, *6*, 256.
(33) Backx, C.; de Groot, C. P. M. *Surf. Sci.* **1982**, *115*, 382.
(34) Backx, C.; de Groot, C. P. M.; Biloen, P.; Sachtler, W. M. H. *Surf. Sci.* **1983**, *128*, 81.
(35) Kruger, B.; Benndorf, C. *Surf. Sci.* **1986** *178*, 704.
(36) Solomon, J. L.; Madix, R. J.; Stohr, J. *J. Chem. Phys.* **1990**, *93*, 8379.
(37) Barteau, M. A.; Madix, R. J. *Surf. Sci.* **1981**, *103*, L171.
(38) Hahn, J. R.; Ho, W. *J. Chem. Phys.* **2005**, *122*, 244704.
(39) Hahn, J. R.; Lee, H. J.; Ho, W. *Phys. Rev. Lett.* **2000**, *85*, 1914.
(40) Hahn, J. R.; Ho, W. Unpublished results.
(41) Scheiner, S.; Grabowski, S. J.; Kar, T. *J. Phys. Chem. A* **2001**, *105*, 10607.
(42) Chattopadhyay, S.; Plummer, P. L. M. *J. Chem. Phys.* **1990**, *93*, 4187.